NEIL1 stimulates neurogenesis and suppresses neuroinflammation after stress

Beimeng Yang[a], **David M. Figueroa**[a], **Yujun Hou**[a], **Mansi Babbar**[a], **Stephanie L. Baringer**[a], **Deborah L. Croteau**[a], **Vilhelm A. Bohr**[a,b,*]

[a]Laboratory of Molecular Gerontology, National Institute on Aging, National Institutes of Health, Baltimore, MD, 21224, USA

[b]Danish Center for Healthy Aging, University of Copenhagen, 2200, Copenhagen, Denmark

Abstract

Cellular exposure to ionizing radiation leads to oxidatively generated DNA damage, which has been implicated in neurodegenerative diseases. DNA damage is repaired by the evolutionarily conserved base excision repair (BER) system. Exposure of mice to ionizing radiation affects neurogenesis and neuroinflammation. However, the consequences of deficient DNA repair on adult neurogenesis and neuroinflammation are poorly understood despite their potential relevance for homeostasis. We previously reported that loss of NEIL1, an important DNA glycosylase involved in BER, is associated with deficiencies in spatial memory, olfaction, and protection against ischemic stroke in mice. Here, we show that Neil1$^{-/-}$ mice display an anxiety-mediated behavior in the open field test, a deficient recognitive memory in novel object recognition and increased neuroinflammatory response under basal conditions. Further, mice lacking NEIL1 have decreased neurogenesis and deficient resolution of neuroinflammation following gamma irradiation (IR)-induced stress compared to WT mice. Neil1$^{-/-}$ IR-exposed mice also exhibit increased DNA damage and apoptosis in the hippocampus. Interestingly, behavioral tests two weeks after IR showed impaired stress response in the Neil1$^{-/-}$ mice. Our data indicate that NEIL1 plays an important role in adult neurogenesis and in the resolution of neuroinflammation.

Keywords

NEIL1; Neuroinflammation; Neurogenesis; DNA damage; DNA microarray

1. Introduction

Ionizing radiation from terrestrial sources is constantly an unprotected risk to humans [1]. Exposure of humans to radiation occurs through medical radiation and global radiation

---

sources. The biological impact of radiation on humans has been reported through the last century but recently there has been growing interest in understanding the effect of radiation exposure to the CNS [2]. Cellular exposure to ionizing radiation leads to oxidizing events inducing the formation of hydroxyl radical (•OH) [3]. Ionizing radiation generates a multiplicity of radical events within a cellular target including in DNA. This includes clustered lesions that may consist of a broad spectrum of DNA damage[4,5]. Irradiation-induced DNA damage is detrimental to the cell unless efficiently repaired. Damaged DNA is repaired by several DNA repair pathways, and one of the most important ones, is base excision repair (BER).

Previous studies have suggested that irradiation-induced neurodegeneration is associated with the depression of hippocampal neurogenesis and neuroinflammation in adult mice [6–8]. Whole-body low-dose IR of mice led to molecular changes in the brain that are similar to those seen in aging and AD [9]. Therefore, IR may be a meaningful tool for examining the relationships between adult neurogenesis, neuroinflammation, and neurodegenerative diseases.

Adult neurogenesis was first reported in 1965, and this observation changed the perception that the mammalian brain was incapable of generating new neurons [10]. New neurons are generated throughout life in two regions of brain, the subventricular zone lining the lateral ventricles and the subgranular zone of the dentate gyrus in the hippocampus [11]. The process of adult neurogenesis begins with generating neurons from NSCs and neural progenitor cells. The rate of neurogenesis can be altered by many factors including age, hormonal status, neuroinflammation and environmental factors, such as radiation [12]. Importantly, alterations in adult neurogenesis have been proposed as a hallmark feature in several neurodegenerative diseases [13].

An important connection between neurodegeneration and neurogenesis is neuroinflammation [14,15]. Neuroinflammation is a process in which the brain clears damaged cells or removes infectious agents [16], and is characterized by the activation of the microglia and astrocytes [17]. Activated microglia and astrocytes are marked by an increase in proliferation, morphological changes, and the release of several inflammatory molecules such as cytokines, reactive oxygen species, and nitric oxide [15]. An appropriate neuroinflammatory response can promote brain homeostasis [18] while excessive neuroinflammation can inhibit neuronal regeneration. In general, it appears that chronic neuroinflammation negatively regulates neurogenesis [19,20].

Defective repair of nuclear or mitochondrial DNA damage has been implicated in several neurodegenerative disorders [21]. Oxidatively generated DNA damage is largely repaired by the evolutionarily conserved BER system. NEIL1, an important DNA glycosylase, is a versatile DNA repair enzyme because it can recognize DNA lesions in ssDNA, dsDNA, and bubble DNA substrates [22]. It is well-documented that the most biologically relevant NEIL1 substrates consist of oxidized pyrimidine and formamidopyrimidine lesions [23]. NEIL1 also interacts with many proteins involved in DNA replication and DNA repair [24,25]. These proteins include XRCC1, WRN, PCNA, CSB and RAD9 [26]. NEIL1 has been shown to localize to mitochondria and nuclei [27] suggesting it contributes to DNA

repair in both compartments. NEIL1 may be implicated in the removal of oxidized pyrimidine bases, such as 5,6-dihydroxy-5,6-dihydrothymine from complex clustered DNA damage generated from IR, attenuating their harmful effects. NEIL1 has also been implicated in learning and memory, olfaction, and protection against ischemic injury in murine neurons [28,29].

Loss of BER is involved in the progression of aging and neurodegenerative diseases [30,31]. In this study, we report a role for NEIL1 in neurogenesis and neuroinflammation following stress in the form of 6 Gy whole-body IR. We show that neurogenesis and resolution of neuroinflammation in the hippocampus from $Neil1^{-/-}$ mice is deficient after IR stress. We further find that DNA damage and apoptosis markers are increased in $Neil1^{-/-}$ IR-exposed mice. Moreover, $Neil1^{-/-}$ mice show an impaired stress response in behavioral tests 2–4 weeks after IR. Combined, these results demonstrate that a BER deficiency adversely modulates recovery from IR stress in the central nervous system.

2. Materials and methods

2.1. Mice

All mice were maintained in the in a constant-temperature facility with a 12 h light/12 h dark cycle and given food and water ad libitum. The mice were a generous gift from Steven Lloyd (Oregon Health and Science University, Portland, OR). The mice were backcrossed on a C57BL/6 background. Male littermate wild type (28–42 weeks old) and male $Neil1^{-/-}$ mice were used for all experiments. All procedures were approved by the Animal Care and Use Committee of the National Institute on Aging Intramural Research Program.

2.2. Gamma irradiation

Mice were subjected to whole body gamma irradiation in a Nordion Gammacell 40 Exactor Irradiator. Mice were placed in a stereotaxic cube box and exposed to gamma irradiation or not irradiated (sham). Radiation (6 Gy) was delivered at a rate of 0.74 Gy/min on day 0. After exposure, mice were returned to home cages.

2.3. BrdU injections

BrdU (Sigma) was dissolved in 0.9% NaCl and sterile filtered at 0.2 μm. Mice were administered intraperitoneally BrdU injection (100 mg/kg) before and after 2 h of IR exposure. Mice were sacrificed at 20 h or four weeks after IR.

2.4. RNA purification and microarray

Gene expression analysis was performed using mouse cortex. RNA was purified with PureLink™ RNA isolation kit following manufacturer's protocol (Thermo). RNA concentration and purity were conducted using a NanoDrop ND-1000 spectrophotometer. The quality of the RNA was inspected using a 2100 Bioanalyzer (Agilent Technologies). Samples with RNA integrity less than 7.5 were discarded. Finally, we used n=4 for each group for analysis. The microarray was performed by the Gene expression and Genomics core facility (NIA) and analyzed using DIANE 6.0 software as described before [32]. A gene was considered significant if the absolute value of its z-ratio was ≥ 1.5, p-value ≤ 0.05. A

complete set of 880 canonic pathways and 2392 chemical perturbation gene sets were obtained from the Molecular Signatures Database (MSigDB, Broad Institute, Massachusetts Institute of Technology, MA, USA). The complete set was tested for Geneset enrichment using parametric analysis of gene set enrichment (PAGE). Raw microarray hybridization intensity data were filtered to remove undetected and array control probes, before computing log z-score for each sample to identify and exclude possible outlying samples via clustering, scatter plots, and principal components analysis. After removal of the outlying samples, a sample-specific quantile normalization of the filtered raw average signal was employed to yield quantile normalized log scale z-scores. These quantile z-scores were used to ensure a standard normal distribution in further statistical analysis, including ANOVA, t- and z-testing. Z-ratio values of ± 1.5 were used as cut-off values and calculated using a combination of thresholds, including $p <$ value 0.05, 30% FDR, and average signal intensity of comparison >0. The gene expression change z-ratio values were then used as input to perform PAGE testing. For each gene set change, an aggregate z-score, and p-value with false discovery change was calculated and reported for statistical significance. The accession number for the raw and processed microarray data reported in this paper is GEO: GSE130034.

2.5. Immunofluorescence staining

Mice were perfused with 4% paraformaldehyde (4% paraformaldehyte in 0.1 M phosphate buffer) then placed in 30% sucrose (Sigma) in phosphate buffered saline until sunken at 4 °C. Brains were cryoprotected in tissue freezing medium, and 30 μm-coronal sections were obtained with a cryostat CM 3080S (Leica). Primary antibodies, including rat anti-BrdU (Abcam, 1:500), rabbit anti-Ki67 (Millipore, 1:500) were used for immunostaining. Sectioned tissue into 30-mm coronal slices using a cryostat. Transfered sections to 24-well plates loaded with 0.1 M PBS (pH 7.4), including 0.02% sodium azide. Collected six sets of sections per brain. Typically, we collect 60–70 sections per dentate gyrus, and so there are 10–12 sections per set. Brain slices were incubated with 4′,6-diaminodino-2-phenylindole (DAPI, Invitrogen, 1:2000) for 15 min before mounting onto slides. For thymidine glycol (TG): the slices were performed antigen retrieval by incubation in 0.01 mol/l sodium citrate (pH 6.0, sigma) at 95 °C for 20 min. The primary anti-TG monoclonal antibody specific for TG in DNA polymers (mouse IgG1kappa) was purchased from the Adipogen. The entire dentate gyrus was scanned using an Axiovert 200 M Zeiss microscope (Zeiss) equipped with AxioVision 4.8.3.0 software.

2.6. Culture and exposure of NSCs

Neural stem cells (NSCs) were isolated from embryonic mice cortex, cultured and expanded. Cortical regions of embryos (E13.5–14.5) were dissected and dissociated with 0.05% trypsin/EDTA, and then titrated through a 40 μm cell-filter to ensure single cells. Cells were then centrifuge and resuspended in starting medium (DMEM/Ham's F-12 nutrient solution + GlutaMAX (Gibco, #10565018), 50 U/ml penicillin, 50 μg/ml streptomycin, 0.25 μg/ml amphotericin B (Gibco, #15290018), 2% B27 (Thermo Fisher Scientific, #17504001), 20 ng/ml epidermal growth factor (EGF) and 10 ng/ml fibroblast growth factor 2 (FGF-2) (R&D Systems, #028-EG-200 and #3139-FB-025/CF, respectively), and seeded at a density of 200,000 cells/ml. Cells were grown in starting medium at 37 °C, with 5% CO2. Half of

the medium was changed every other day. After seven days of growth, passage 1, neural stem cells were dissociated using NeuroCult Chemical Dissociation kit following the manufacturer's protocol (StemCell Technologies, #05707). Cells were resuspended in starting medium and seeded out for continual exposure experiments. Cells were seeded in 96-well plates for 24 h. Then cells were irradiated with a series of gamma irradiation at a rate of 0.74 Gy/min in a Nordion Gammacell 40 Exactor Irradiator.

2.7. NSCs proliferation assay

A CCK-8 kit (Dojindo) was used to measure proliferation of neural stem cells. Briefly, 10 μl of the kit reagent were added to the cells that had been treated as described above in 96-well plates, followed by a 2 h incubation. Cell proliferation was assessed using a spectrophotometer plate reader measuring the absorbance at 450 nm. All results were adjusted by subtracting the optical densities (ODs) measured from an identically conditioned well without cells. For cytotoxicity assay, a colorimetric assay kit (Dojindo) was used according to the manufacturer 's instructions to quantify the LDH released from the cultured neural stem cells. Cytotoxicity was assessed using a spectrophotometer plate reader by measuring absorbance at 490 nm. All results were adjusted by subtracting the OD of an identical well without cells.

2.8. Western blotting

Mouse hippocampi were lysed in RIPA buffer (Sigma) including a protease/phosphatase stop cocktail (Sigma). Protein concentrations were measured by BCA assay (Thermo) and lysates (20 μg per lane) were separated on a 4–15% SDS-PAGE (Thermo) and transferred onto a PVDF membrane. The membrane was incubated with blocking solution (5% milk (BD) in TBST) for 1 h at room temperature, followed by overnight incubation with a primary antibody at 4 °C. The membrane was incubated with HRP-conjugated secondary antibody (Cell signaling) for 1 h at room temperature. Immunoreactivity was detected with an ECL kit (Millipore, or Thermo). Optical density of the immunoreactivity bands was analyzed using Image J software (NIH).

2.9. Antibodies

Rabbit anti-IL6 (Abcam), goat anti- IL10 (Proteintech), rabbit anti-β-actin (Cell signaling), mouse anti-BCL2 (Santa cruz), Rabbit anti-Ace-P53 (Cell signaling), rabbit anti-PAR (Trevigen), Rabbit anti-PARP1 (Cell signaling), mouse anti-P53 (Santa cruz), mouse anti-γH2AX (Abclonal), goat anti-SOX2 (R&D), goat anti-IBA1 (Novus), rabbit anti-GFAP (Millipore), rabbit anti-NFκB-P50 (Proteintech), rabbit anti-Cl-Caspase3 (Cell signaling), and Rabbit anti-Nestin (Millipore). HRP-conjugated secondary antibodies (Cell signaling).

2.10. Cytokine array

Mouse eye bleeds were collected in EDTA treated tubes. After centrifugation, the supernatant was flash frozen. Plasma diluted-1:2 was used to detect cytokines and chemokines by use of 31-Plex Cytokine/Chemokine array (Eve Technologies).

2.11. Open field test

Each individual mouse was placed in the center of open field box (40 cm×40 cm×40 cm) and recorded for 20 min. The center zone was set up as a 26.6–cm^2 area from the peripheral walls. Travel distance and time spent in the center were measured and recorded by ANY-maze software (Stoelting).

2.12. Elevated plus maze test

The test was performed as previously reported [32]. A mouse was placed in a device with two open arms (30×5×2.5 cm) and two closed arms (30×5×15 cm) and recorded for a period of 5 min. The time spent in each arm was tracked by the ANY-maze software (Stoelting).

2.13. Novel object recognition

Before training, mice were handled 1–2 min per day for 3 days prior to beginning behavioral assessment. During the training phase, mice were put in the experimental box (27.5cm×27.5cm×25cm) and were exposed to two identical objects for 10 min. After 1 h, mice were put back into the same box, which had been modified to contain one familiar object and one novel object. To exclude olfactory cues, the boxes and objects were cleaned before each test. The automatic tracking system (Anymaze, Stoelting) was used to monitor exploration behavior. Exploration time and the percent of time mice spent with the old object and the novel object was measured.

2.14. Fear conditioning test

The context fear conditioning test was carried out by using operant chambers (Med Associates) with an electrifiable steel grid floor. During training phase, mice were habituated to the chamber for 2 min, followed by 3 times electrical foot shock (0.5 mA) with 1-min intervals. 24 h after training, the mice were placed in same chamber for 5 min and their freezing behavior was measured.

2.15. Forced swim test

In the forced swim test, mice were placed in a plastic beaker (17.5 cm diameter, 24 cm high), filled with water (22 °C) to a height of 15 cm for 6 min. The time mice spent floating (immobility time) during the last 4 min as well as the latency to the first immobility episode were manually observed. The movement of mice were record and analyzed by automatic tracking system (Anymaze, Stoelting).

2.16. Y-maze

The maze consisted of three arms (8×30×15 cm), with an angle of 120 degrees between each arm. The numbers of entries and alterations were recorded using the Anymaze tracking system. Mice were put on the center of the Y maze and allowed them to freely explore the maze for 5min. The arms were cleaned with 70% ethanol solution between different mice. Spontaneous alternation percentage (SAP) is calculated by the number of actual alternations/ (total arm entries-2) X 100.

2.17. Statistical analysis

P values < 0.05 are considered statistically significant (*P < 0.05, **P < 0.01, ***P < 0.001). All results are presented as means ± SEM and were analyzed with Statview Software. Statistical differences between two groups were measured by Student's *t*-test. Multiple groups were assessed by one-way ANOVA.

3. Results

3.1. Neil1$^{-/-}$ mice are more susceptible to IR damage

Based on prior literature [33] and on our own experience, we used 6 Gy IR to induce whole-body DNA damage. This dose is not lethal but high enough to have an effect. We divided mice in 4 groups: WT sham, WT IR, Neil1$^{-/-}$ sham, and Neil1$^{-/-}$ IR. Mice were sacrificed 20 h or 28 days after IR exposure following treatment paradigm (Fig. 1A). All mice were alive after this sublethal dose of IR, with no obvious visual macroscopic effects. Changes in the body weight of mice exposed to IR or sham are shown (Fig. 1B). Both WT and Neil1$^{-/-}$ mice lost more weight over the follow-up period after IR exposure than without, however, irradiated Neil1$^{-/-}$ mice lost more weight than the irradiated WT mice. This suggest that Neil1$^{-/-}$ mice are more sensitive to IR than their WT littermates.

Gene expression array analysis was performed to get unbiased insights into pathways affected by IR. Here we analyzed the PAGE of the curated canonical pathway via BioCarta, KEGG, and Reactome to determine the pathway alterations in the cortex 20 h after IR. Significantly changed pathways were defined as those displaying an absolute z-score of at least 1.5, a p-value 0.05, and a FDR<0.3 and having at least three changed genes in the pathway in at least one genotype [32]. Heatmaps (Fig. 1C–E) show the various pathways changed in WT or Neil1$^{-/-}$ mice exposed to IR or sham in different comparison. Neil1$^{-/-}$ IR mice showed increases in biological oxidation, protein and lipid metabolism when compared to the Neil1$^{-/-}$ sham mice (Fig. 1C). Notably, immune-related death, complement, and the lectin pathways were all increased in Neil1$^{-/-}$ IR vs Neil1$^{-/-}$ sham comparison, but not in WT IR vs WT sham (Fig. 1D). Interestingly, neuronal functional pathways were significantly down-regulated in Neil1$^{-/-}$ IR mice compared to Neil1$^{-/-}$ sham mice (Fig. 1E). Conversely, the neuronal function pathways were uniformly up-regulated in WT IR vs WT sham (Fig. 1E). These results suggest that IR induces more neuronal dysfunction in Neil1$^{-/-}$ mice than WT mice.

3.2. IR decreases neurogenesis in Neil1$^{-/-}$ mice

Adult hippocampal neurogenesis plays an important role in brain function, and evidence suggests that hippocampal neurogenesis is compromised after IR [34]. To quantify newly generated neurons arising from neural progenitor cells, we labeled newborn neurons with BrdU 2 h before and after IR exposure via I.P. injection (Fig. 1A) then imaged the hippocampus 28 days later. We observed that there was a decrease in the number of BrdU positive cells in the dentate gyrus region of the hippocampus in the Neil1$^{-/-}$ IR mice as compared to the Neil1$^{-/-}$ sham, WT sham and WT IR mice (Fig. 2A and B), suggesting decreased neurogenesis in the Neil1$^{-/-}$ IR mice. We also checked proliferating neural progenitor cells by examining the marker Ki67 4-weeks after IR exposure. Interestingly,

Ki67-labeled proliferating cells were increased in the WT IR-exposed mice as compared to WT sham mice, indicating that IR increases proliferation of WT neural progenitor cells (Fig. 2C and D). IR had no effects on proliferation of Neil1$^{-/-}$ neural progenitor cells after 4 weeks of recovery.

To verify this deficit in the NEIL1 defective NSCs, we used NSCs from WT or Neil1$^{-/-}$ embryos to investigate neurogenesis in vitro (Figs. S1A and B). NSCs were exposed to increasing doses of IR and cell proliferation was evaluated using the CCK-8 (Fig. 2E) and the LDH assay (Fig. 2F). IR significantly decreased the proliferation of NSCs in a concentration-dependent manner in WT and Neil1$^{-/-}$ NSCs, and Neil1$^{-/-}$ NSCs were more sensitive to IR than WT NSCs (Fig. 2E and F). Also, we found that exposure to 0.1 Gy of irradiation significantly increased proliferation in WT NSCs, but not Neil1$^{-/-}$ IR NSCs. Combined, our results show that NEIL1 is important for the neurogenesis in vivo and in vitro following IR stress.

3.3.   IR induces an abnormal inflammatory response in Neil1$^{-/-}$ mice

In addition to neurogenesis, irradiation also leads to neuroinflammation in mice [35,36]. Microglia, astrocytes, blood inflammatory cells, and neurons regulate brain inflammation after contusion-induced spinal cord injury [37]. Inflammatory cells protect neurons and repair the damaged microenvironment. We therefore investigated the response of astrocytes and microglia to IR in the hippocampus.

The density of microglia (IBA1) and astrocytes (GFAP) were significantly increased in Neil1$^{-/-}$ sham compared to WT sham mice (Fig. 3A and B), suggesting that Neil1$^{-/-}$ mice have increased basal neuroinflammation. IR increased the astrocyte population in WT mice. However, the signal for IBA1 and GFAP were downregulated by IR exposure in Neil1$^{-/-}$ mice, which is consistent with our gene expression array analysis (Fig. 1E). These results indicate abnormal neuroinflammatory responses in Neil1$^{-/-}$ mice after IR exposure. Cytokines are a major component of the neuroinflammatory response, and thus we measured the expression of the proinflammatory cytokines IL6, IL10 and NFκB-P50 in the hippocampus. Neil1$^{-/-}$ IR mice had elevated levels of IL6 (P=0.055) and IL10 compared to WT sham mice (Fig. 3C and D). NFκB-P50 was significantly increased in Neil1$^{-/-}$ IR in comparison to other groups (Fig. 3C and D).

To quantify circulating pro-inflammatory cytokines, we performed cytokine array from plasma (Fig. 4), to detect MCP-1, MIP2, RANTES, IL-5, TNFα, IL4, IL17, and VEGF. There were no differences between WT sham and Neil1$^{-/-}$ sham mice. However, these cytokines were consistently increased in Neil1$^{-/-}$ IR when compared to Neil1$^{-/-}$ sham (Fig. 4). Collectively, WT mice showed a proficient neuroinflammatory response in the brain and a resolved inflammatory response in blood following IR exposure. In contrast, Neil1$^{-/-}$ mice displayed an abnormal neuroinflammatory response in the hippocampus, and an unresolved, excessive inflammatory response in plasma following IR exposure.

3.4.   IR increases DNA damage and apoptosis in Neil1$^{-/-}$ mice

To further explore neuronal dysfunction, we investigated the expression of DNA damage and apoptosis proteins in mouse hippocampal tissue at 20 h and 4 weeks after IR.

γ-H2AX is a DNA damage marker originally thought to be detecting, but more recently associated much more broadly with DNA damage and genotoxicity marker [38]. At 20 h after IR exposure, the DNA damage marker γ-H2AX and apoptosis marker Cl-Caspase 3 were increased in Neil1$^{-/-}$ IR mice compared to all other groups (Fig. 5A and B). We also measured another biomarker of radiation-induced DNA damage, thymine glycol, which is a substrate for NEIL1 enzyme [39]. Thymine glycol positive cells were significantly increased in Neil1$^{-/-}$ IR mice compared to all other groups at 20 h after IR exposure (Fig. 5C and D). To further assess DNA damage, we analyzed PAR levels. PAR is a post-translational modification found near sites of DNA damage, which is catalyzed by PARP [40]. PAR was increased in Neil1$^{-/-}$ IR when compared with Neil1$^{-/-}$ sham and WT IR mice (Fig. 5E and F). Interestingly, WT IR mice showed less PAR compared to WT sham (Fig. 5E and F). PARP1 can be activated by DNA damage and plays an important role in DNA repair, implicating cleaved-PARP1 in the apoptotic process [41]. There were no significant changes in full length PARP1 protein between the IR and sham groups (Fig. 5E and F), however, cleaved-PARP1 was increased in Neil1$^{-/-}$ IR than in Neil1$^{-/-}$ sham mice (Fig. 5E and F). Additionally, DNA damage activates p53, a transcription factor, through post-translational modifications that include both phosphorylation and acetylation [42]. We found that acetylation of p53 (Ace-p53) and γ-H2AX were increased in the Neil1$^{-/-}$ IR group compared to WT IR and Neil1$^{-/-}$ sham mice (Fig. 5E and F). There was no change in p53 or BCL2 protein levels between the Neil1$^{-/-}$ IR and the Neil1$^{-/-}$ sham group (Fig. 5E and F). These data suggest that a single 6 Gy dose of IR induces Caspase 3 and Ace-p53 dependent apoptotic pathways.

At 4 weeks, PAR levels were increased in the Neil1$^{-/-}$ IR mice compared to the WT sham group (Fig. 6A and B). The Cleaved-PARP1 level was highly expressed in WT IR compared to WT sham (Fig. 6A and B). Since PARP1 uses NAD$^+$ as a substrate, we also measured the total NAD, NAD$^+$, NADH, and NAD$^+$/NADH ratio in all four groups of mice after IR exposure. Neil1$^{-/-}$ IR mice showed decreased NAD+ and decreased total NAD levels compared to WT sham (Fig. 6C). There was no difference in NADH or NAD+/NADH level between Neil1$^{-/-}$ IR and WT sham mice (Fig. 6C). Thus, IR significantly increased the DNA damage and NAD+ depletion in Neil1$^{-/-}$ mice compared to WT mice.

3.5. Neil1$^{-/-}$ IR mice exhibit impaired behavior after stress

IR has a variety of effects on the brain, leading to abnormal behaviors and disease [43–45]. Our results suggest that IR decreased adult neurogenesis, affected neuroinflammation, and increased apoptosis in Neil1$^{-/-}$ mice. Next, we assessed whether these changes impacted behaviors. Thus, we performed a series of behavioral tests that have previously been related to stress. Distance traveled was measured in the open field test to assess motor function. We found that WT IR mice traveled less distance than WT sham and Neil1$^{-/-}$ IR mice, suggesting that WT mice showed less motor function after IR exposure, but that Neil1$^{-/-}$ IR mice did not (Fig. 7A). Anxiety was assessed by time spent in the center of open field (Fig. 7A) and time spent in open arms of elevated plus maze (Fig. 2SA). Neil1$^{-/-}$ sham animals spent less time in the center zone compared to WT sham animals, suggesting that Neil1$^{-/-}$ mice had greater natural anxiety. After IR, WT mice spent less time in the center zone than WT sham mice, indicating increased anxiety (Fig. 7B). Neil1$^{-/-}$mice failed to show this

response to IR. To further evaluate anxiety, we tested mice in the elevated plus maze. In this test, mice spend less time in the open arm if they are more anxious. Compared with WT sham mice, WT IR mice trended to spend less time exploring in the open arms (p=0.052, Fig. 7C). But no change was observed between Neil1$^{-/-}$ sham and Neil1$^{-/-}$ IR mice.

Recognition memory was also tested in these mice via the novel object recognition test. All mice spent similar amounts of time exploring the two identical objects during the training phase. During the test phase, we replaced one object with a novel object. If mice spend more time exploring the novel object than the old object, they have proficient recognition memory. Here we found that WT sham mice spent significantly more time exploring the novel object compared to the WT IR group (Fig. 7D). We also analyzed the percent of exploration time between novel and old object. Only the WT sham group could recognize a novel object from an old object, this was not seen in the WT IR, Neil1$^{-/-}$ sham, Neil1$^{-/-}$ IR (Fig. 7E), suggesting that WT IR, Neil1$^{-/-}$ sham and Neil1$^{-/-}$ IR mice were deficient in recognition memory. Thus Neil1 $^{-/-}$ mice had a defect in recognition memory before stress. Fear memory was measured by the percentage of time freezing in the fear conditioning test. WT IR mice spent significantly more time freezing (Fig. 5F) and had less motion activity (Fig. S2B) than the WT sham and Neil1$^{-/-}$ IR mice, suggesting that WT IR mice have a better fear memory than WT sham. IR had no effects on fear memory in Neil1$^{-/-}$ mice, suggesting that Neil1$^{-/-}$ exhibit an impaired response to IR exposure.

We also measured other behaviors to determine if IR impacted them and if NEIL1 affected them. We measured olfactory function by testing how long the mice took to find a buried food pellet using the buried food test. While more Neil1$^{-/-}$ mice failed (max time 600 s) to find the pellet than WT mice, there were no significant differences in latencies (Figs. S2C and D). Working memory was evaluated by quantifying the percentage of spontaneous alternation in the Y maze test. IR had no effect on the working memory (Fig. S2E). Depression was tested by measuring the immobility time in the forced swimming test. IR induced depression phenotypes in both WT mice and Neil1$^{-/-}$ mice, but there were no differences between WT IR and Neil1$^{-/-}$ IR (Fig. S2F). Overall, Neil1$^{-/-}$ mice show an anxiety-mediated behavior (Fig. 7B) in the open field test, a deficient recognitive memory in novel object recognition test (Fig. 7E) and declined olfaction (Fig. S2D) under basal condition. In summary, Neil1$^{-/-}$ mice display impaired behavioral responses to IR compared to WT mice (Fig. 7A–C and 7F).

4. Discussion

Here we demonstrate that NEIL1 plays an important role in adult neurogenesis, resolution of neuroinflammation, neuroprotection and related behaviors in mice following IR exposure. IR induces oxidative stress and produces a large quantity of ROS in organisms. ROS is also generated endogenously during mitochondrial respiration. ROS inflicts oxidative damage on macromolecules, including DNA [46–48]. Oxidatively generated DNA damage is elevated in neurons during normal aging or in neurodegenerative diseases, which may result in impaired expression or dysfunction of proteins that play critical roles in neurogenesis, synaptic plasticity and memory [49,50].

BER is the major pathway for the repair of oxidative stress induced DNA base lesions [51,52]. Some major DNA glycosylases recognize and remove oxidatively modified bases from DNA, including OGG1, NTH1, and NEIL1 [53]. We have reported that thymine glycol and 5-hydroxyuracil incision capacity were significantly lower in nuclear and mitochondrial lysates in brain tissue samples from Neil1$^{-/-}$ mice compared with WT mice [29]. These data suggest that these two pyrimidine base oxidation products are substrates for NEIL1 enzymes. The biological relevance of these lesions is not clear. Some studies have reported that NEIL1 also recognize the secondary oxidation products of 8-oxo-7, 8-dihydroguanine including spiroiminodihydantoin, guanidinohydantoin and carboxamido-5-formamido-2-iminohydantoin [54–57].

Radiation-induced clustered DNA lesions, also called multiply damaged sites, are a hallmark of ionizing radiation. They include a multitude of DNA lesions. When the BER pathway is insufficient, the observed hierarchy in the processing of the lesions within a cluster leads to the formation of SSB or DSB [58]. In this study, we assessed the effect of NEIL1 absence on radiation-induced DNA damage in hippocampus. Thymine glycol is a representative oxidized pyrimidine base and is also an excellent substrate for NEIL1 enzyme. We found that thymine glycol positive cells in hippocampus were significantly increased in Neil1$^{-/-}$ IR mice (Fig. 5C and D). Complex DSBs, either formed directly by irradiation or by the processing of non-DSBs clustered lesions, activate the DNA damage responses and repair signaling cascades that modulate cell cycle arrest, DNA repair, and cell fates. γ-H2AX is a DNA damage marker originally thought to be specifically detecting DSBs marker, but more recently associated broadly with DNA damage. While assessing this marker is not a direct measure for NEIL1 function following IR exposure, it reflects the biological relevance of NEIL1 in this context (Fig. 5A and B).

Radiation-induced cognitive deficits are associated with the reduction of hippocampal neurogenesis and abnormal neuroinflammation in adult mice [6]. Previously, Raber et al. reported that 10 Gy X-ray led to significant and prolonged loss of proliferating cells after irradiating the dentate gyrus in adult mice [8]. However, another study demonstrated that a 2 Gy dose of whole-body irradiation showed transient damage to neurogenesis which persisted for 3 days [34]. We should point out that NEIL3 was also shown to be activated during the S-phase [59]. Another study reported that NEIL3 is required for adult neurogenesis to counteract cognitive defects [60]. However, human NEIL3's substrate preference has not been well characterized. It is possible that NEIL3 also is involved in adult neurogenesis for a different set of oxidized bases. Here, we found that adult neurogenesis in Neil1$^{-/-}$ IR mice was decreased compared to Neil1$^{-/-}$ sham mice at 20 h after IR exposure (Fig. 2A and B). This suggests that a 6 Gy dose of whole-body IR showed a transient decline in neurogenesis. Interestingly, Ki67 labeled cells, a marker for proliferating cells, are increased in WT IR mice compared to WT sham, but not in Neil1$^{-/-}$ IR (Fig. 2C and D). Increased neurogenesis may be essential for increased adult hippocampal stress resistance [61]. Low dose irradiation exposure has been shown to confer neuroprotection and activate reparative mechanisms [62,63]. In accordance with the increased neurogenesis in WT IR mice (Fig. 2C and D), we found that a 0.1 Gy dose of IR increased WT NSCs proliferation in vitro (Fig. 2E and F), but there was a failed response in Neil1$^{-/-}$ NSCs. Hegde et al. reported that NEIL1 is critical for efficient repair of oxidized DNA base damage and enhanced cell survival [46]. They also

showed that NEIL1 depletion inhibits DNA replication fork progression after oxidative stress [64]. Consistent with those reports, we demonstrate that NEIL1 is important for neurogenesis in vivo and for proliferation in vitro after IR stress.

In addition to neurogenesis, brain inflammation plays a detrimental role in the pathogenesis of neurodegenerative disorders like Alzheimer's disease (AD) and Parkinson's Disease [65,66]. Cytokines are pleiotropic molecules with important roles in inflammation. Pro-inflammatory cytokines and neuroinflammation not only participate in the inflammatory response, but are also involved in neurogenesis and neuroprotection [67]. Cranial irradiation causes inflammation in the hippocampus [68] and decreased neurogenesis [43]. Microglia, neutrophils, monocytes, astrocytes, and neurons contribute to brain inflammation, suggesting that these cells protect precious neurons in the brain from secondary injury [37]. Here, we find that neuroinflammation was increased in Neil1$^{-/-}$ mice under basal conditions, and that IR reduced the astrocyte and microglial populations in Neil1$^{-/-}$ mice (Fig. 3). This suggests that NEIL1 contributes to the resolution of neuroinflammation, and that loss of NEIL1 results in abnormal neuroinflammatory responses after stress in the CNS. Also, increased pro-inflammatory cytokines were detected in Neil1$^{-/-}$ IR mice compared to WT sham (Fig. 4), WT IR and Neil1$^{-/-}$ sham mice, suggesting that Neil1$^{-/-}$ mice have an excessive inflammatory response after IR exposure in blood. Interestingly, statistically significant increases in induction of both pro- and anti-inflammatory cytokines were observed in hippocampal tissue and blood of Neil1$^{-/-}$ IR mice (Fig. 3C and D, Fig. 4). A recent study also reported increased pro- and anti-inflammatory cytokines in UVB-exposed NEIL1$^{-/-}$mouse skin. This mixed pro- and anti-inflammatory environment likely led to increased oxidative stress in the hippocampus and formation of ROS-induced DNA base lesions. In accordance with this hypothesis, we detect decreased NAD+ and total NAD levels in irradiated Neil1$^{-/-}$ tissues (Fig. 6). We also observed that DNA damage and apoptosis was increased in Neil1$^{-/-}$ irradiated mice, and we detected more NAD+ depletion in Neil1$^{-/-}$ mice following IR. We believe that the increased DNA damage by IR leads to more NAD + depletion in Neil1$^{-/-}$ mice, possibly via increased parylation (Fig. 5), a substrate of NAD+. Thus, loss of NEIL1 may contribute to DNA damage and NAD + consumption.

In order to investigate the effects of abnormal neurogenesis, neuroinflammation, and neuronal degeneration on brain functions, we examined several behaviors related to stress responses in the mice. Here, we found that Neil1$^{-/-}$ sham mice were more anxious in the open field test compared to WT sham mice (Fig. 7B). In addition, recognition memory was deficient in Neil1$^{-/-}$ sham mice compared to WT sham (Fig. 7D and E). Other BER deficient mice, lacking XRCC1 or OGG1, showed no cognitive deficits [69,70], suggesting that NEIL1 may be particularly important in preserving cognitive function. This is also supported by observations that NEIL1 is decreased in AD patients [71]. A previous study suggested that most irradiation induced changes in behavior are transient and rapid [72]. Here, we checked the effects of IR stress on mouse behavior 2–4 weeks after exposure. Neil1$^{-/-}$ IR mice displayed a lack of stress response in the open field test (Fig. 7A and B) and in the context fear conditioning test (Fig. 7F) compared to WT IR mice. Interestingly, fear memory was improved in the WT IR mice compared to WT sham, with no change in Neil1$^{-/-}$ IR mice (Fig. 7F). Also Reid et al. reported that enhanced fear memory was observed in whole body X ray irradiation of mice [73]. Therefore, we believe that IR induces

the activation of astrocytes, which could confer neuroprotection, increased hippocampal neurogenesis and enhancement of fear memory in WT mice. This response has been referred to as radiation homeostasis, where exposure to a minor stressor can induce protective mechanisms [45,74]. In contrast, the Neil1$^{-/-}$ mice did not show any benefits from an IR-induced response resulting in failed changes in fear memory.

In summary, the data presented here reveal an important role of NEIL1 in protecting the brain against IR-induced stress and cognitive dysfunction. Our results clearly show that loss of NEIL1 may affect neurogenesis, resolution of neuroinflammation, neuronal functions and various behavioral measures. DNA repair is important for healthy aging and in response to stress, and this study expands the neuronal and behavioral features that can be modulated by loss of an important DNA repair protein like NEIL1.

Supplementary Material

Refer to Web version on PubMed Central for supplementary material.

Acknowledgments

Abbreviations:

NEIL1	Endonuclease VIII-like 1
BER	base excision repair
•OH	hydroxyl radical
DSBs	double strand breaks
IR	gamma irradiation
NSCs	neural stem cells
FDR	false-discovery rate
XRCC1	X-ray repair cross-complementing protein 1
WRN	RecQ helicase-like
PCNA	proliferating cell nuclear antigen
CSB	Cockayne syndrome group B
AD	Alzheimer's disease

PAGE	parametric Analysis of Gene Set Enrichment
CCK-8	cell counting kit
LDH	lactic acid dehydrogenase
PAR	poly (ADP-ribose)
PARP	poly (ADP-ribose) polymerase
ROS	reactive oxygen species

References

[1]. Sharma NK, Sharma R, Mathur D, Sharad S, Minhas G, Bhatia K, Anand A, Ghosh SP, Role of ionizing radiation in neurodegenerative diseases, Front. Aging Neurosci. 10 (2018).

[2]. Valentin J, Low-dose extrapolation of radiation-related cancer risk, Ann. ICRP 35 (4) (2005) 1–140.

[3]. Azzam EI, Jay-Gerin J-P, Pain D, Ionizing radiation-induced metabolic oxidative stress and prolonged cell injury, Cancer Lett. 327 (1–2) (2012) 48–60. [PubMed: 22182453]

[4]. Watanabe R, Rahmanian S, Nikjoo H, Spectrum of radiation-induced clustered non-DSB damage– A Monte Carlo track structure modeling and calculations, Radiat. Res. 183 (5) (2015) 525–540. [PubMed: 25909147]

[5]. Sage E, Shikazono N, Radiation-induced clustered DNA lesions: repair and mutagenesis, Free Radic. Biol. Med. 107 (2017) 125–135. [PubMed: 27939934]

[6]. Rola R, Fishman K, Baure J, Rosi S, Lamborn KR, Obenaus A, Nelson GA, Fike JR, Hippocampal neurogenesis and neuroinflammation after cranial irradiation with 56Fe particles, Radiat. Res. 169 (6) (2008) 626–632. [PubMed: 18494546]

[7]. Snyder J, Hong N, McDonald R, Wojtowicz J, A role for adult neurogenesis in spatial long-term memory, Neuroscience 130 (4) (2005) 843–852. [PubMed: 15652983]

[8]. Raber J, Rola R, LeFevour A, Morhardt D, Curley J, Mizumatsu S, VandenBerg SR, Fike JR, Radiation-induced cognitive impairments are associated with changes in indicators of hippocampal neurogenesis, Radiat. Res. 162 (1) (2004) 39–47. [PubMed: 15222778]

[9]. Lowe XR, Bhattacharya S, Marchetti F, Wyrobek AJ, Early brain response to low-dose radiation exposure involves molecular networks and pathways associated with cognitive functions, advanced aging and Alzheimer's disease, Radiat. Res. 171 (1) (2009) 53–65. [PubMed: 19138050]

[10]. Altman J, Das GD, Autoradiographic and histological evidence of postnatal hippocampal neurogenesis in rats, J. Comp. Neurol. 124 (3) (1965) 319–335. [PubMed: 5861717]

[11]. Zhao C, Deng W, Gage FH, Mechanisms and functional implications of adult neurogenesis, Cell 132 (4) (2008) 645–660. [PubMed: 18295581]

[12]. Li J, Meng Z, Zhang G, Xing Y, Feng L, Fan S, Fan F, Buren B, Liu Q, N-acetylcysteine relieves oxidative stress and protects hippocampus of rat from radiation-induced apoptosis by inhibiting caspase-3, Biomed. Pharmacother. 70 (2015) 1–6. [PubMed: 25776470]

[13]. Palop JJ, Chin J, Mucke L, A network dysfunction perspective on neurodegenerative diseases, Nature 443 (7113) (2006) 768. [PubMed: 17051202]

[14]. Amor S, Woodroofe MN, Innate and adaptive immune responses in neurodegeneration and repair, Immunology 141 (3) (2014) 287–291. [PubMed: 23758741]

[15]. Fuster-Matanzo A, Llorens-Martín M, Hernández F, Avila J, Role of Neuroinflammation in Adult Neurogenesis and Alzheimer Disease: Therapeutic Approaches, Mediators of Inflammation 2013, (2013).

[16]. Schmidt OI, Heyde CE, Ertel W, Stahel PF, Closed head injury—an inflammatory disease? Brain Res. Rev. 48 (2) (2005) 388–399. [PubMed: 15850678]

[17]. Streit WJ, Walter SA, Pennell NA, Reactive microgliosis, Prog. Neurobiol. 57 (6) (1999) 563–581. [PubMed: 10221782]

[18]. Molina-Holgado E, Molina-Holgado F, Mending the broken brain: neuroimmune interactions in neurogenesis, J. Neurochem. 114 (5) (2010) 1277–1290. [PubMed: 20534007]

[19]. Fan L-W, Pang Y, Dysregulation of neurogenesis by neuroinflammation: key differences in neurodevelopmental and neurological disorders, Neural Regen. Res. 12 (3) (2017) 366. [PubMed: 28469641]

[20]. Russo MV, McGavern DB, Inflammatory neuroprotection following traumatic brain injury, Science 353 (6301) (2016) 783–785. [PubMed: 27540166]

[21]. Jeppesen DK, Bohr VA, Stevnsner T, DNA repair deficiency in neurodegeneration, Prog. Neurobiol. 94 (2) (2011) 166–200. [PubMed: 21550379]

[22]. Popuri V, Croteau DL, Bohr VA, Substrate specific stimulation of NEIL1 by WRN but not the other human RecQ helicases, DNA Repair 9 (6) (2010) 636–642. [PubMed: 20346739]

[23]. Wallace SS, DNA glycosylases search for and remove oxidized DNA bases, Environ. Mol. Mutagen. 54 (9) (2013) 691–704. [PubMed: 24123395]

[24]. Theriot CA, Hegde ML, Hazra TK, Mitra S, RPA physically interacts with the human DNA glycosylase NEIL1 to regulate excision of oxidative DNA base damage in primer-template structures, DNA Repair 9 (6) (2010) 643–652. [PubMed: 20338831]

[25]. Hegde ML, Theriot CA, Das A, Hegde PM, Guo Z, Gary RK, Hazra TK, Shen B, Mitra S, Physical and functional interaction between human oxidized base-specific DNA glycosylase NEIL1 and flap endonuclease 1, J. Biol. Chem. 283 (40) (2008) 27028–27037. [PubMed: 18662981]

[26]. Panigrahi SK, Hopkins KM, Lieberman HB, Regulation of NEIL1 protein abundance by RAD9 is important for efficient base excision repair, Nucleic Acids Res. 43 (9) (2015) 4531–4546. [PubMed: 25873625]

[27]. Hu J, de Souza-Pinto NC, Haraguchi K, Hogue BA, Jaruga P, Greenberg MM, Dizdaroglu M, Bohr VA, Repair of formamidopyrimidines in DNA involves different glycosylases role OF the OGG1, NTH1, and NEIL1 enzymes, J. Biol. Chem. 280 (49) (2005) 40544–40551. [PubMed: 16221681]

[28]. Canugovi C, Misiak M, Scheibye-Knudsen M, Croteau DL, Mattson MP, Bohr VA, Loss of NEIL1 causes defects in olfactory function in mice, Neurobiol. Aging 36 (2) (2015) 1007–1012. [PubMed: 25448603]

[29]. Canugovi C, Yoon JS, Feldman NH, Croteau DL, Mattson MP, Bohr VA, Endonuclease VIII-like 1 (NEIL1) promotes short-term spatial memory retention and protects from ischemic stroke-induced brain dysfunction and death in mice, Proceedings of the National Academy of Sciences, 2012, p. 201204156.

[30]. Weissman L, Jo D-G, Sørensen MM, de Souza-Pinto NC, Markesbery WR, Mattson MP, Bohr VA, Defective DNA base excision repair in brain from individuals with Alzheimer's disease and amnestic mild cognitive impairment, Nucleic Acids Res. 35 (16) (2007) 5545–5555. [PubMed: 17704129]

[31]. Wilson DM III, Bohr VA, The mechanics of base excision repair, and its relationship to aging and disease, DNA Repair 6 (4) (2007) 544–559. [PubMed: 17112792]

[32]. Hou Y, Lautrup S, Cordonnier S, Wang Y, Croteau DL, Zavala E, Zhang Y, Moritoh K, O'Connell JF, Baptiste BA, NAD+ supplementation normalizes key Alzheimer's features and DNA damage responses in a new AD mouse model with introduced DNA repair deficiency, Proc. Natl. Acad. Sci. Unit. States Am. 115 (8) (2018) E1876–E1885.

[33]. Haridas S, Kumar M, Manda K, Chronic melatonin administration mitigates behavioral dysfunction induced by γ-irradiation, Horm. Behav. 62 (5) (2012) 621–627. [PubMed: 23026539]

[34]. Kim J-S, Lee H-J, Kim JC, Kang SS, Bae C-S, Shin T, Jin J-K, Kim SH, Wang H, Moon C, Transient impairment of hippocampus-dependent learning and memory in relatively low-dose of acute radiation syndrome is associated with inhibition of hippocampal neurogenesis, J. Radiat. Res. 49 (5) (2008) 517–526. [PubMed: 18574327]

[35]. Kempf SJ, Casciati A, Buratovic S, Janik D, von Toerne C, Ueffing M, Neff F, Moertl S, Stenerlöw B, Saran A, The cognitive defects of neonatally irradiated mice are accompanied by changed synaptic plasticity, adult neurogenesis and neuroinflammation, Mol. Neurodegener. 9 (1) (2014) 57. [PubMed: 25515237]

[36]. Moravan MJ, Olschowka JA, Williams JP, O'Banion MK, Cranial irradiation leads to acute and persistent neuroinflammation with delayed increases in T-cell infiltration and CD11c expression in C57BL/6 mouse brain, Radiat. Res. 176 (4) (2011) 459–473. [PubMed: 21787181]

[37]. Jeong H-K, Ji K, Min K, Joe E-H, Brain inflammation and microglia: facts and misconceptions, Exp. Neurobiol. 22 (2) (2013) 59–67. [PubMed: 23833554]

[38]. Garcia-Canton C, Anadon A, Meredith C, Assessment of the in vitro γH2AX assay by high content screening as a novel genotoxicity test, Mutat. Res. Genet. Toxicol. Environ. Mutagen 757 (2) (2013) 158–166.

[39]. Onizuka K, Yeo J, David SS, Beal PA, NEIL1 binding to DNA containing 2'-fluorothymidine glycol stereoisomers and the effect of editing, Chembiochem : Eur. J. Chem. Biol. 13 (9) (2012) 1338–1348.

[40]. Zong W-X, Ditsworth D, Bauer DE, Wang Z-Q, Thompson CB, Alkylating DNA damage stimulates a regulated form of necrotic cell death, Genes Dev. 18 (11) (2004) 1272–1282. [PubMed: 15145826]

[41]. Chaitanya GV, Alexander JS, Babu PP, PARP-1 cleavage fragments: signatures of cell-death proteases in neurodegeneration, Cell Commun. Signal. 8 (1) (2010) 31. [PubMed: 21176168]

[42]. Sakaguchi K, Herrera JE, Saito S.i., Miki T, Bustin M, Vassilev A, Anderson CW, Appella E, DNA damage activates p53 through a phosphorylation–acetylation cascade, Genes Dev. 12 (18) (1998) 2831–2841. [PubMed: 9744860]

[43]. Lazarini F, Mouthon M-A, Gheusi G, De Chaumont F, Olivo-Marin J-C, Lamarque S, Abrous DN, Boussin FD, Lledo P-M, Cellular and behavioral effects of cranial irradiation of the subventricular zone in adult mice, PLoS One 4 (9) (2009) e7017. [PubMed: 19753118]

[44]. Naylor AS, Bull C, Nilsson MK, Zhu C, Björk-Eriksson T, Eriksson PS, Blomgren K, Kuhn HG, Voluntary running rescues adult hippocampal neurogenesis after irradiation of the young mouse brain, Proc. Natl. Acad. Sci. Unit. States Am. 105 (38) (2008) 14632–14637.

[45]. Betlazar C, Middleton RJ, Banati RB, Liu G-J, The impact of high and low dose ionising radiation on the central nervous system, Redox Biol. 9 (2016) 144–156. [PubMed: 27544883]

[46]. Hegde ML, Hegde PM, Arijit D, Boldogh I, Mitra S, Human DNA glycosylase NEIL1's interactions with downstream repair proteins is critical for efficient repair of oxidized DNA base damage and enhanced cell survival, Biomolecules 2 (4) (2012) 564–578. [PubMed: 23926464]

[47]. Klaunig JE, Xu Y, Isenberg JS, Bachowski S, Kolaja KL, Jiang J, Stevenson DE, Walborg EF Jr., The role of oxidative stress in chemical carcinogenesis, Environ. Health Perspect. 106 (suppl 1) (1998) 289–295. [PubMed: 9539021]

[48]. Shokoohinia Y, Hosseinzadeh L, Moieni-Arya M, Mostafaie A, Mohammadi-Motlagh H-R, Osthole attenuates doxorubicin-induced apoptosis in PC12 cells through inhibition of mitochondrial dysfunction and ROS production, BioMed Res. Int. (2014) 2014.

[49]. Hamilton A, Holscher C, The effect of ageing on neurogenesis and oxidative stress in the APPswe/PS1deltaE9 mouse model of Alzheimer's disease, Brain Res. 1449 (2012) 83–93. [PubMed: 22418058]

[50]. Wu A, Ying Z, Gomez-Pinilla F, Dietary curcumin counteracts the outcome of traumatic brain injury on oxidative stress, synaptic plasticity, and cognition, Exp. Neurol. 197 (2) (2006) 309–317. [PubMed: 16364299]

[51]. Harrison JF, Hollensworth SB, Spitz DR, Copeland WC, Wilson GL, LeDoux SP, Oxidative stress-induced apoptosis in neurons correlates with mitochondrial DNA base excision repair pathway imbalance, Nucleic Acids Res. 33 (14) (2005) 4660–4671. [PubMed: 16107556]

[52]. Karahalil B, Hogue BA, De Souza-pinto NC, BOHR VA, Base excision repair capacity in mitochondria and nuclei: tissue-specific variations, FASEB J. 16 (14) (2002) 1895–1902. [PubMed: 12468454]

[53]. Ide H, Kotera M, Human DNA glycosylases involved in the repair of oxidatively damaged DNA, Biol. Pharm. Bull. 27 (4) (2004) 480–485. [PubMed: 15056851]

[54]. Krishnamurthy N, Zhao X, Burrows CJ, David SS, Superior removal of hydantoin lesions relative to other oxidized bases by the human DNA glycosylase hNEIL1, Biochemistry 47 (27) (2008) 7137–7146. [PubMed: 18543945]

[55]. Popuri V, Croteau DL, Bohr VA, Substrate specific stimulation of NEIL1 by WRN but not the other human RecQ helicases, DNA Repair 9 (6) (2010) 636–642. [PubMed: 20346739]

[56]. Alshykhly OR, Fleming AM, Burrows CJ, Guanine oxidation product 5-carboxamido-5-formamido-2-iminohydantoin induces mutations when bypassed by DNA polymerases and is a substrate for base excision repair, Chem. Res. Toxicol. 28 (9) (2015) 1861–1871. [PubMed: 26313343]

[57]. Shafirovich V, Kropachev K, Kolbanovskiy M, Geacintov NE, Excision of oxidatively generated guanine lesions by competing base and nucleotide excision repair mechanisms in human cells, Chem. Res. Toxicol. 32 (4) (2019) 753–761. [PubMed: 30688445]

[58]. Sage E, Shikazono N, Radiation-induced clustered DNA lesions: repair and mutagenesis, Free Radic. Biol. Med. 107 (2017) 125–135. [PubMed: 27939934]

[59]. Neurauter CG, Luna L, Bjørås M, Release from quiescence stimulates the expression of human NEIL3 under the control of the Ras dependent ERK–MAP kinase pathway, DNA Repair 11 (4) (2012) 401–409. [PubMed: 22365498]

[60]. Regnell CE, Hildrestrand GA, Sejersted Y, Medin T, Moldestad O, Rolseth V, Krokeide SZ, Suganthan R, Luna L, Bjørås M, Hippocampal adult neurogenesis is maintained by Neil3-dependent repair of oxidative DNA lesions in neural progenitor cells, Cell Rep. 2 (3) (2012) 503–510. [PubMed: 22959434]

[61]. Levone BR, Cryan JF, O'Leary OF, Role of adult hippocampal neurogenesis in stress resilience, Neurobiol. Stress 1 (2015) 147–155. [PubMed: 27589664]

[62]. Yoshimoto M, Kataoka T, Toyota T, Taguchi T, Yamaoka K, Inhibitory effects of prior low-dose X-irradiation on cold-induced brain injury in mouse, Inflammation 35 (1) (2012) 89–97. [PubMed: 21258855]

[63]. Otani A, Kojima H, Guo C, Oishi A, Yoshimura N, Low-dose-rate, low-dose irradiation delays neurodegeneration in a model of retinitis pigmentosa, Am. J. Pathol. 180 (1) (2012) 328–336. [PubMed: 22074737]

[64]. Hegde ML, Hegde PM, Bellot LJ, Mandal SM, Hazra TK, Li G-M, Boldogh I, Tomkinson AE, Mitra S, Prereplicative repair of oxidized bases in the human genome is mediated by NEIL1 DNA glycosylase together with replication proteins, Proc. Natl. Acad. Sci. Unit. States Am. 110 (33) (2013) E3090–E3099.

[65]. Ekdahl CT, Claasen J-H, Bonde S, Kokaia Z, Lindvall O, Inflammation is detrimental for neurogenesis in adult brain, Proc. Natl. Acad. Sci. Unit. States Am. 100 (23) (2003) 13632–13637.

[66]. Nelson PT, Soma LA, Lavi E, Microglia in diseases of the central nervous system, Ann. Med. 34 (7) (2002) 491–500. [PubMed: 12553488]

[67]. Kim Y-K, Na K-S, Myint A-M, Leonard BE, The role of pro-inflammatory cytokines in neuroinflammation, neurogenesis and the neuroendocrine system in major depression, Prog. Neuro Psychopharmacol. Biol. Psychiatr. 64 (2016) 277–284.

[68]. Monje ML, Mizumatsu S, Fike JR, Palmer TD, Irradiation induces neural precursor-cell dysfunction, Nat. Med. 8 (9) (2002) 955. [PubMed: 12161748]

[69]. Klungland A, Rosewell I, Hollenbach S, Larsen E, Daly G, Epe B, Seeberg E, Lindahl T, Barnes DE, Accumulation of premutagenic DNA lesions in mice defective in removal of oxidative base damage, Proc. Natl. Acad. Sci. Unit. States Am. 96 (23) (1999) 13300–13305.

[70]. McNeill DR, Lin P-C, Miller MG, Pistell PJ, de Souza-Pinto NC, Fishbein KW, Spencer RG, Liu Y, Pettan-Brewer C, Ladiges WC, XRCC1 haploinsufficiency in mice has little effect on aging, but adversely modifies exposure-dependent susceptibility, Nucleic Acids Res. 39 (18) (2011) 7992–8004. [PubMed: 21737425]

[71]. Sliwinska A, Sitarek P, Toma M, Czarny P, Synowiec E, Krupa R, Wigner P, Bialek K, Kwiatkowski D, Korycinska A, Decreased expression level of BER genes in Alzheimer's disease patients is not derivative of their DNA methylation status, Prog. Neuro Psychopharmacol. Biol. Psychiatr. 79 (2017) 311–316.

[72]. Bogo V, Effects of bremsstrahlung and electron radiation on rat motor performance, Radiat. Res. 100 (2) (1984) 313–320. [PubMed: 6494442]

[73]. Olsen RH, Weber SJ, Akinyeke T, Raber J, Enhanced cued fear memory following post-training whole body irradiation of 3-month-old mice, Behav. Brain Res. 319 (2017) 181–187. [PubMed: 27865918]

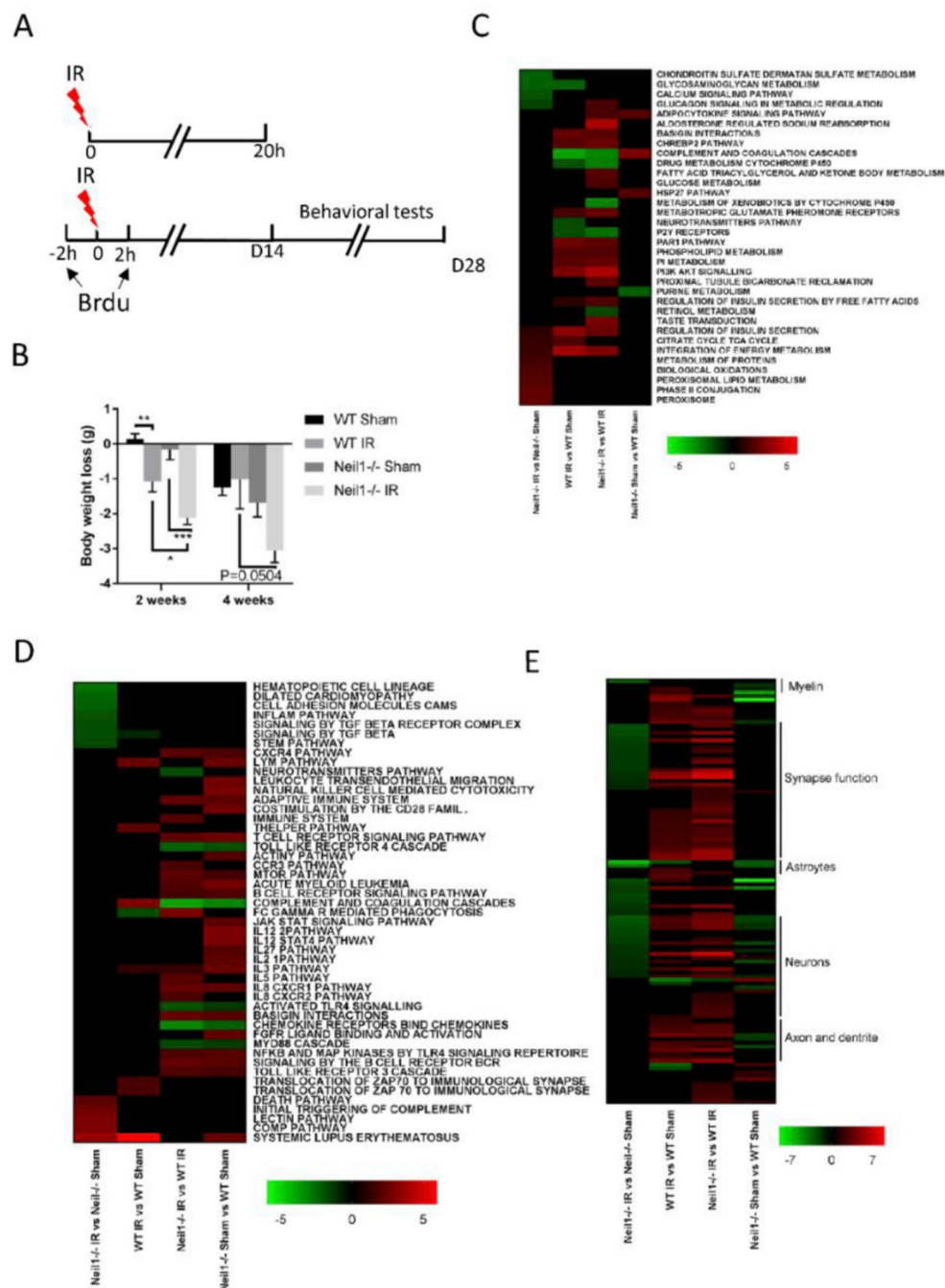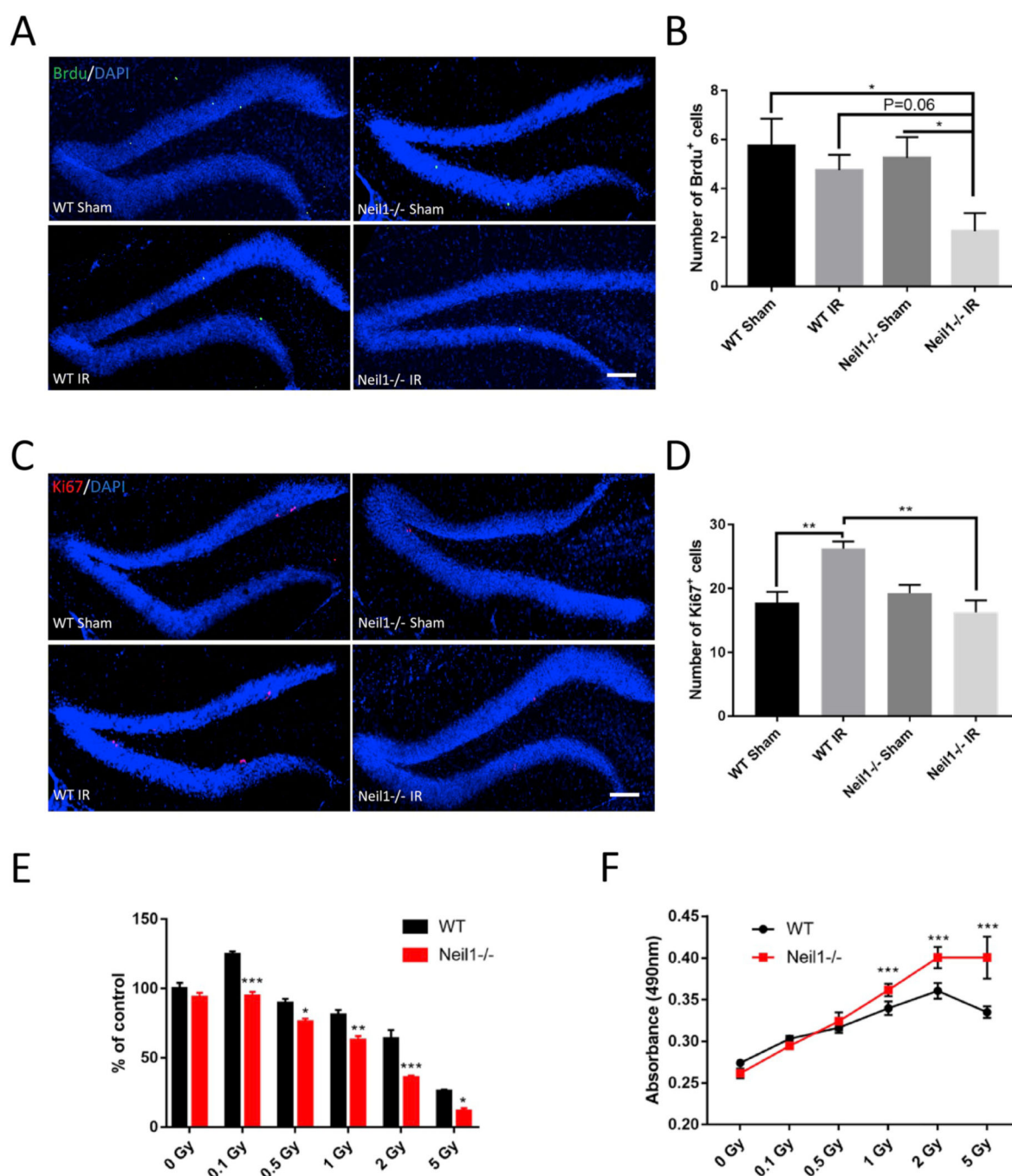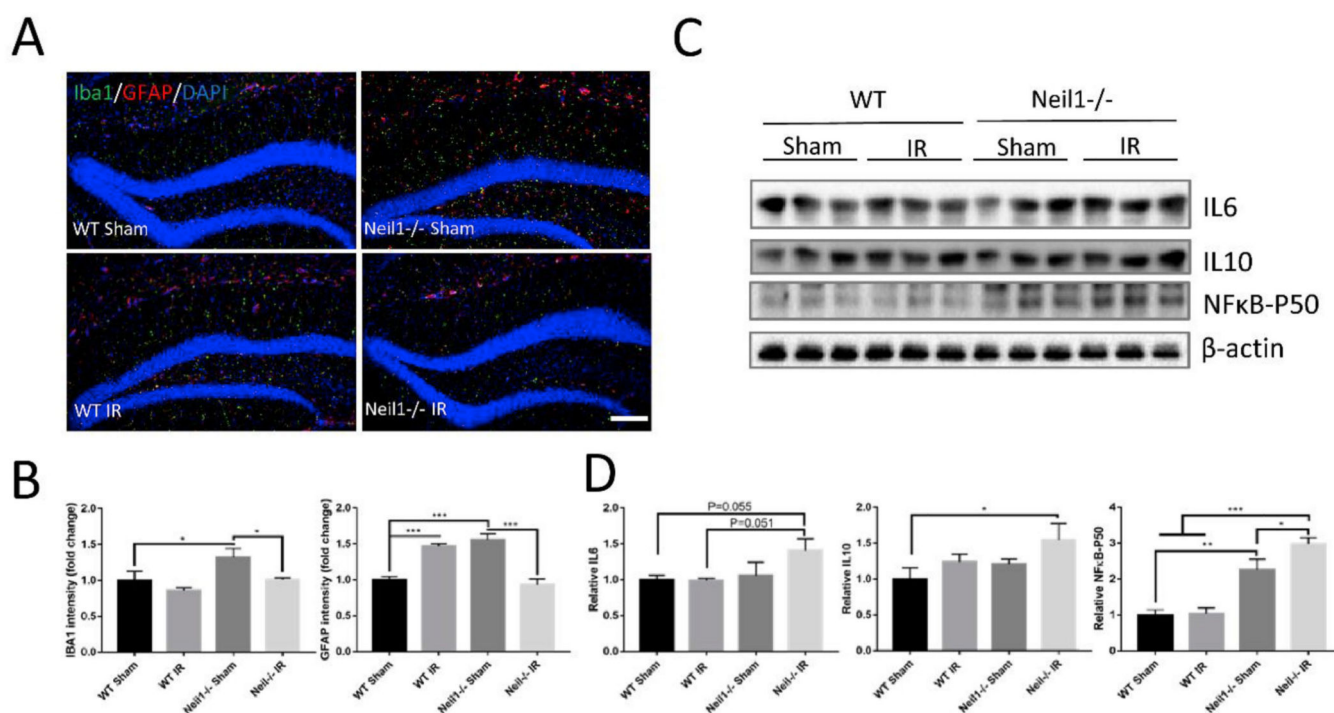[74]. Luckey TD, Physiological benefits from low levels of ionizing radiation, Health Phys. 43 (6) (1982) 771–789. [PubMed: 6759465]

Fig. 1.
Neil1$^{-/-}$ mice are more sensitive to IR exposure. (A) A diagram of the experimental design. (B) Effects of gamma irradiation on the weight loss of WT or Neil1$^{-/-}$ mice. n = 12 (WT sham), 15 (WT IR), 10 (Neil1$^{-/-}$ sham), 13 (Neil1$^{-/-}$ IR) mice. Data shown are mean ± SEM. *P < 0.05, **P < 0.01, ***P < 0.001. Pathways in the hippocampus of IR- and sham-treated mice of WT or Neil1$^{-/-}$ were compared. We divided the pathways into metabolism pathways (C), immune-related pathways (D), and neuronal-related pathways (E).

Fig. 2.
IR decreased neurogenesis in Neil1$^{-/-}$ mice and NSCs. Representative images of BrdU (A) and Ki67 (C) staining of the dentate gyrus sections from WT or Neil1$^{-/-}$ mice after 4 weeks ± IR. Scalebar means 100 μm. Quantification of BrdU (B) and Ki67 (D) positive cells from sections as in (A, C). Cell viability by CKK-8 assay in WT or Neil1$^{-/-}$ NSCs after 24 h of a series of IR exposure (E). Cell toxicity by LDH assay in WT or Neil1$^{-/-}$ NSCs after 24 h of a series of IR exposure (F). Data shown are mean ± SEM. *P < 0.05, **P < 0.01, ***P < 0.001.

Fig. 3.

Neil1$^{-/-}$ mice exhibit increased inflammation response after IR exposure. Representative images of IBA1 (green) and GFAP (red)staining of hippocampi from WT and Neil1$^{-/-}$ mice with or without IR exposure(A). Scalebar means 100 μm. Quantification of IBA1 and GFAP signal intensity (B) from sections was measured. n = 4 mice per group. Quantifications are presented as mean ± SEM. Representative immunoblots of cytokine IL6, IL10 and NFκB-P50 protein from the hippocampi of WT or Neil1$^{-/-}$ mice after 20 h of IR exposure (C). Quantification of IL6, IL10 and NFκB-P50 protein intensity (D). n = 3 mice per group. Data shown are mean ± SEM. *P < 0.05, **P < 0.01, ***P < 0.001. (For interpretation of the references to color in this figure legend, the reader is referred to the Web version of this article.)
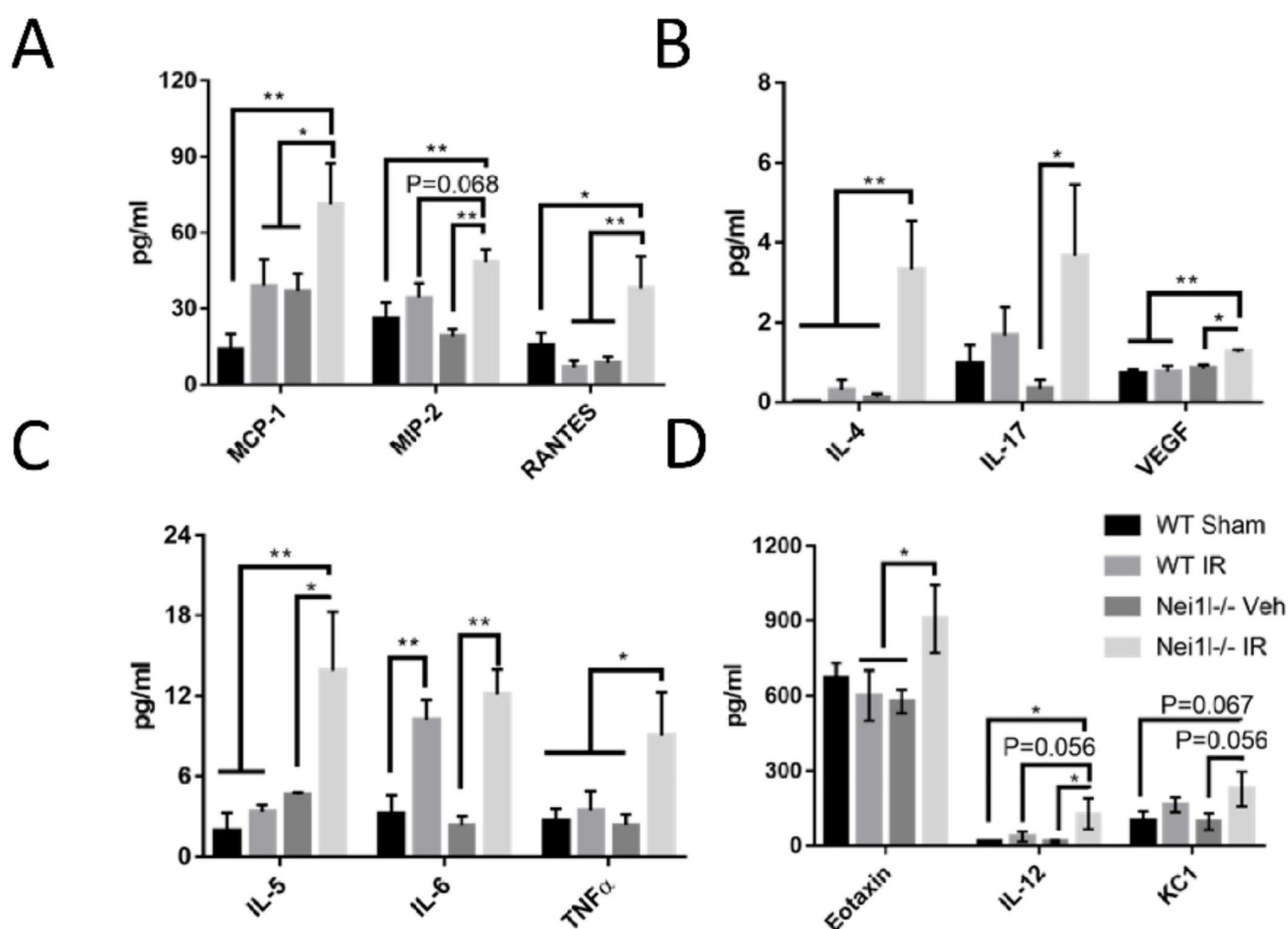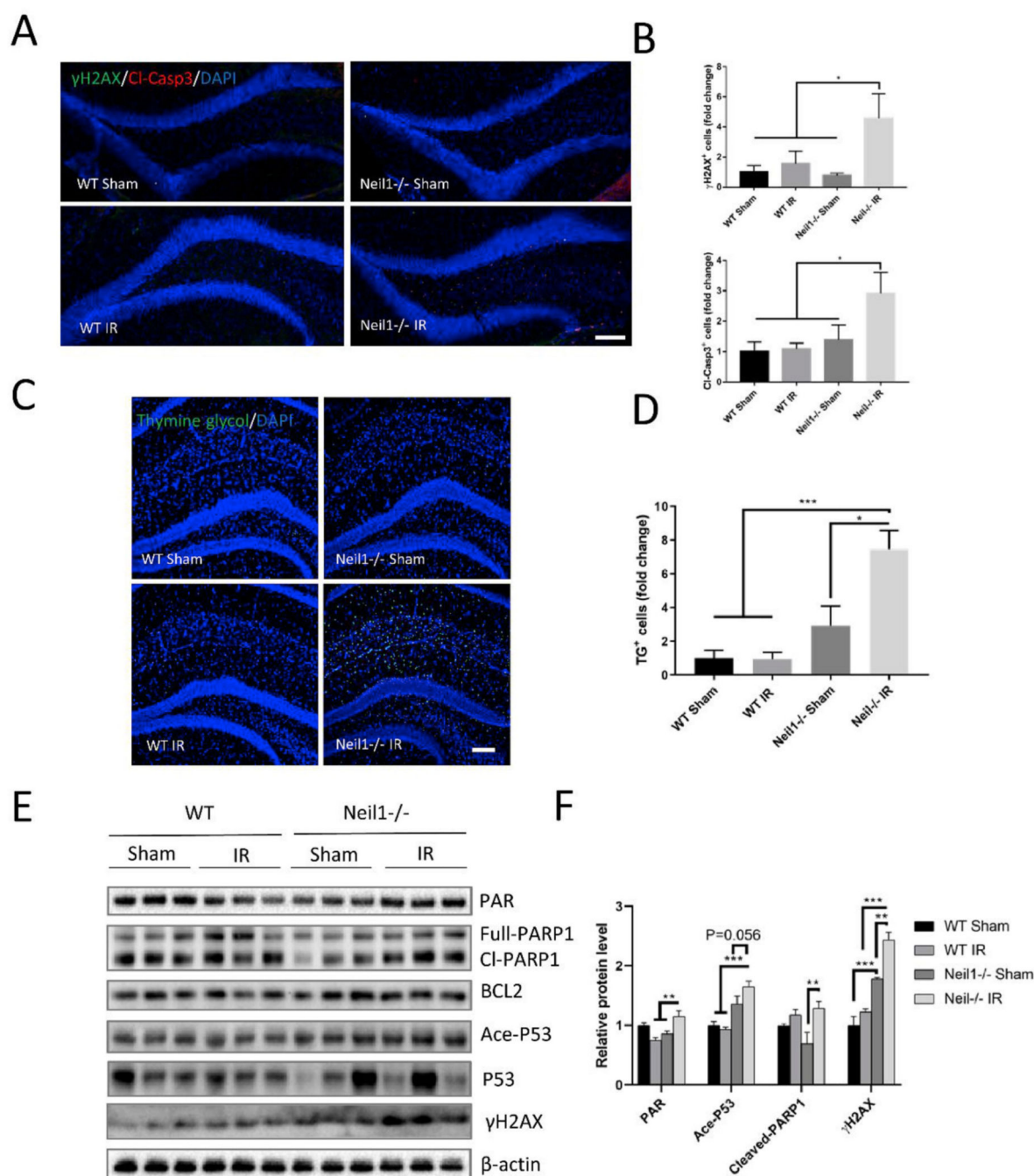
Fig. 4.
Effects of IR on the levels of cytokines in the plasma. (A) MCP-1, MIP-2, RANTES; (B) IL-4, IL17, VEGF; (C)IL-5, IL-6, TNFα; (D) Eotaxin, IL-12, KC1. Data shown are mean ± SEM. n = 5 in WT sham, n = 6 in WT IR, n = 5 in Neil1$^{-/-}$ sham, and n = 5 in Neil1$^{-/-}$ IR. n = 6 in WT IR. *P < 0.05, **P < 0.01, ***P < 0.001.

Fig. 5.

DNA damage and apoptosis are increased in Neil1$^{-/-}$ after 20 h of IR exposure. Representative images of γ-H2AX (green), cleaved-caspase 3 (red), and DAPI (blue) staining of dentate gyrus sections from WT, Neil1$^{-/-}$ mice treated with or without IR (A). Scalebar means 100 μm. Quantification of γH2AX + cells and cleaved-caspase3+ cells in dentate gyrus of hippocampus (B). n = 4 mice per group. Representative images of thymine glycol positive cells (TG$^+$, green), and DAPI (blue) staining of hippocampus sections from WT and Neil1$^{-/-}$ mice treated with or without IR (C). Scalebar is 100 μm. Quantification of

TG + cells in hippocampus (D). Representative immunoblots of the indicated proteins from the hippocampus of WT, and Neil1$^{-/-}$ after 20 h of IR exposure (E). Quantification of immunoblots from Fig. 4C of the PAR, Ace-P53, Cleaved-PARP1, and γ-H2AX protein levels (F). Relative proteins were normalized with β-actin. n = 3 mice per group. Data shown are mean ± SEM. *P < 0.05, **P < 0.01, ***P < 0.001. (For interpretation of the references to color in this figure legend, the reader is referred to the Web version of this article.)
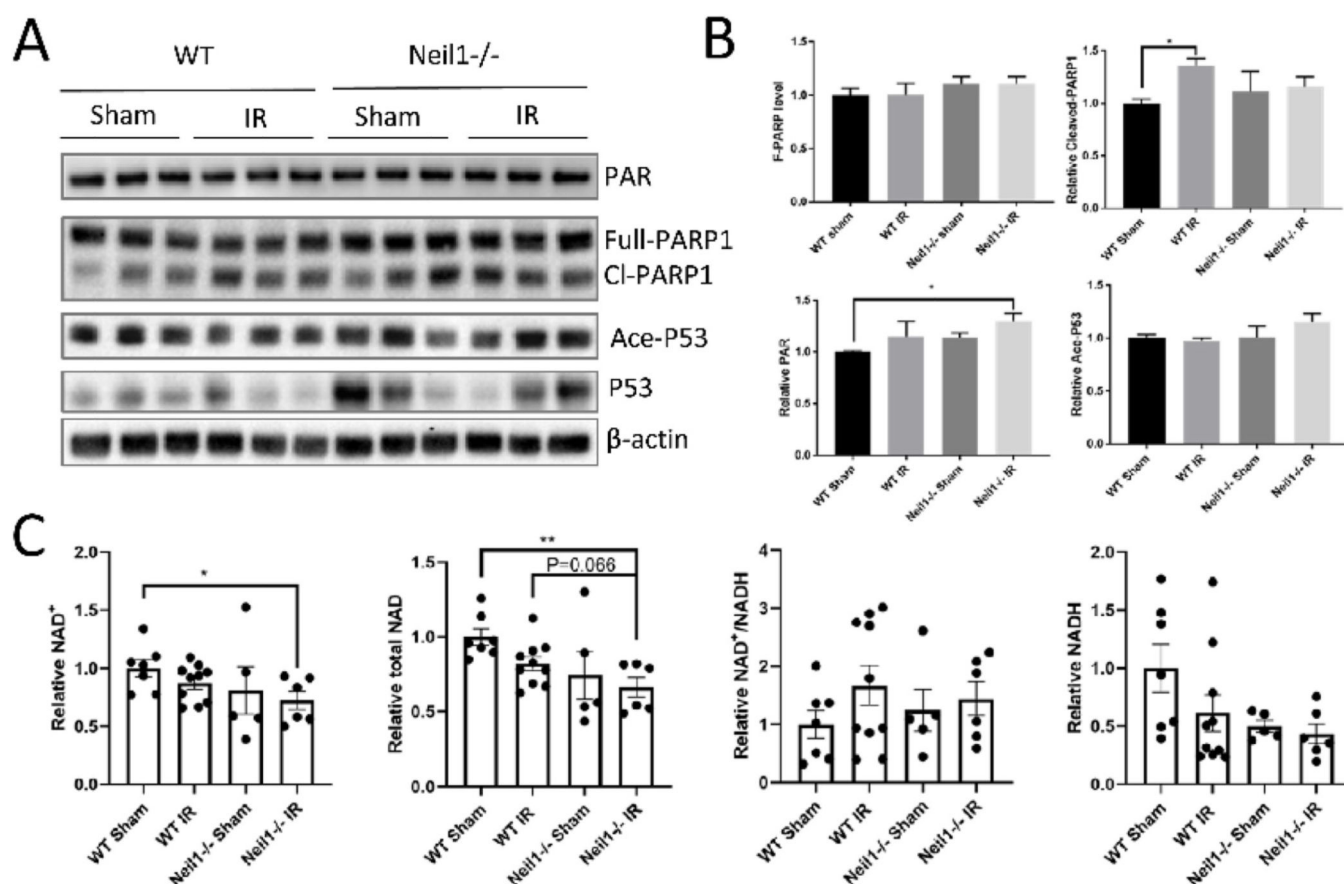
Fig. 6.
DNA damage is increased in Neil1^{−/−} after 4 weeks of IR exposure. Representative immunoblots of the indicated proteins from the hippocampi of WT, and Neil1 [−/−] after 4 weeks of IR exposure (A). Quantification of immunoblots of the PAR, Ace-P53, Cleave-PARP1, Full-PARP1 proteins level (B). Relative proteins were normalized with β-actin. n = 3 mice per group. Data shown are mean ± SEM. *P < 0.05, **P < 0.01, ***P < 0.001. NAD +, total NAD, NADH, and NAD +/NADH ratio in cortex tissue of WT, Neil1^{−/−} at 4 weeks after IR exposure (C). n=7 WT sham, 10 WT IR, 5 Neil1^{−/−} sham, 6 Neil1^{−/−} IR mice. Data shown are mean ± SEM. *P < 0.05, **P < 0.01, ***P < 0.001.
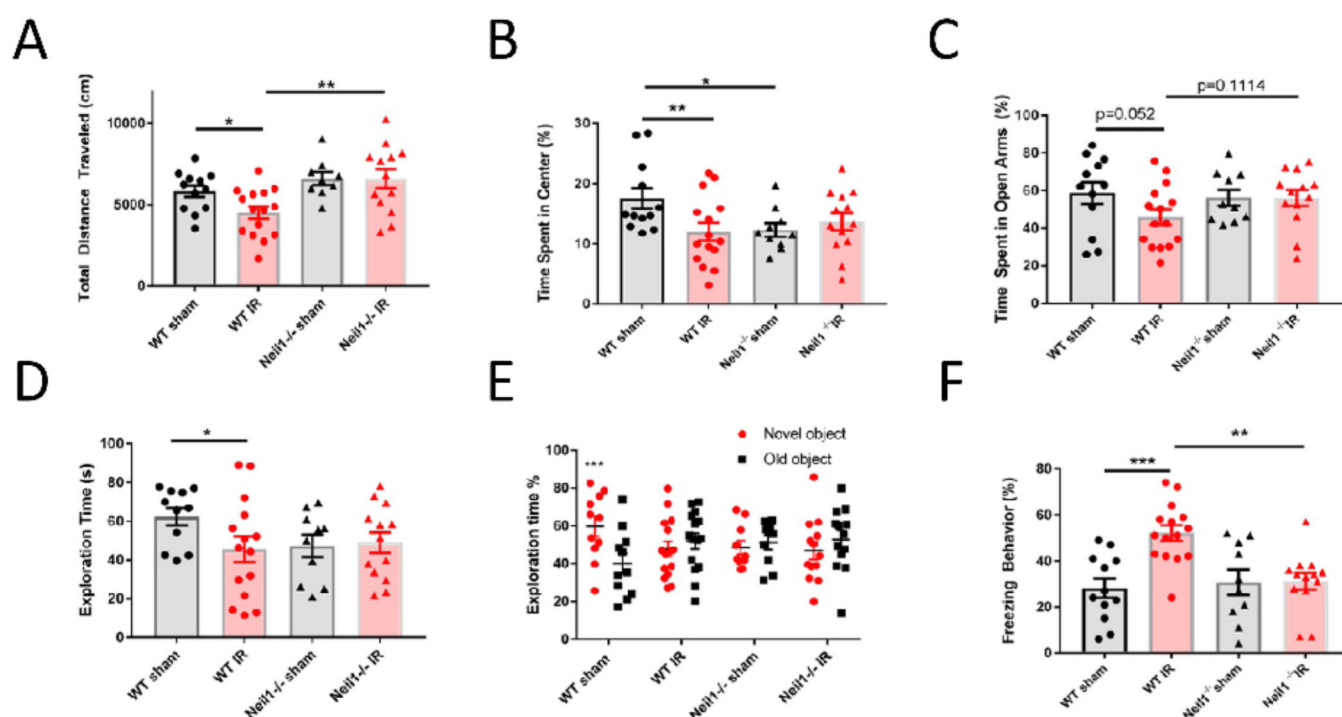
Fig. 7.
Neil1$^{-/-}$ mice show an impaired response to IR compare to WT mice in the behavioral tests. Effects of IR on total distance(A) and time spent in the center (B) in the open field test, the percent of spent time (C) in open arms in elevated plus maze, the exploration time (D) and the percent of exploration time (E) in the novel object recognition test, and the freezing time (F) in context fear conditioning test. Data shown are mean ± SEM. *P < 0.05, **P < 0.01, ***P < 0.001. n = 12 (WT sham), 15 (WT IR), 10 (Neil1$^{-/-}$ sham), 13 (Neil1$^{-/-}$ IR) mice.